α-Sheet: The Toxic Conformer in Amyloid Diseases?

VALERIE DAGGETT

Department of Medicinal Chemistry, University of Washington, Seattle, Washington 98195-7610

Received April 27, 2006

ABSTRACT

A novel secondary structure, the α-sheet, was identified through molecular dynamics (MD) simulations of various proteins associated with amyloid diseases under amyloidogenic conditions. The structure was first predicted by Pauling and Corey, and it has been directly observed in crystal structures of "nonnatural peptides". There are occurrences of α-strands and α-sheets in the Protein Data Bank, but they are rare. We propose that α-sheet is formed during the conformational changes associated with amyloidosis and that it may represent the toxic conformer. Here, structural properties of the α-sheet, background information, and experimental support for this novel structure are presented. Finally we speculate about the possible role of this conformation in disease.

1. Introduction

There are now approximately 25 different human amyloid diseases, each linked to the buildup of a specific precursor protein or peptide.[1] These diseases involve the conversion of a protein from its soluble native state into insoluble amyloid fibrils or, in the case of peptides, conversion from a soluble, loosely structured form to fibrils. Given that many different sequences can form amyloid fibrils of similar architecture, albeit at low resolution, there may be some common structural features of the prefibrillar amyloidogenic intermediates. It has been shown by synchrotron X-ray fiber diffraction that insoluble amyloid fibrils are composed of cross β-sheet structure.[2] Therefore, it has been widely held that the formation of amyloid fibrils involves a transition to β-sheet structure in the amyloidogenic intermediate. However, the mechanism of self-assembly at the atomic level remains elusive. Another twist is that soluble oligomeric intermediates, not the insoluble well-ordered fibrils, are responsible for cellular toxicity.[3,4] Furthermore, it is the soluble oligomeric forms of the prion protein that harbor infectivity.[5] As such, fibrils may be protective, at least up to a point, as their breakdown to smaller aggregates yields greater toxicity and infectivity. The discovery of a compound that promotes inclusions while reducing toxicity and cellular pathology supports this idea.[6] Thus, it behooves us to better understand the structural attributes of the soluble oligomers and their monomeric amyloidogenic precursors.

An antibody was recently identified that is specific for soluble oligomeric intermediates derived from a variety of peptides and proteins, including Aβ42, α-synuclein, islet amyloid polypeptide, polyglutamine, lysozyme, human insulin, and a prion peptide (residues 106–126).[7,8] The antibody does not, however, bind the corresponding insoluble fibrils nor the soluble precursor proteins.[7,8] Based on the specificity of the antibody for soluble oligomers with various sequences, it was proposed that it recognizes a unique toxic conformation of the backbone.[7,8]

Interestingly, this antibody inhibits toxicity associated with the intermediates, implying a common mechanism of toxicity and the hopes of a broad-based therapeutic agent.[7] If there are structural similarities in the toxic forms of different proteins, one wonders whether this might be true with respect to infectivity, as well, and whether other amyloid diseases will prove to be transmissible like prion diseases. Most see this possibility as remote, but Lundmark and co-workers[9] showed that aggregated forms of amyloid protein A, which deposits in vital organs in patients with rheumatoid arthritis and other chronic inflammatory diseases, extracted from diseased mice promotes amyloid formation when administered orally to healthy mice. Transmissibility by cross-seeding with exogeneous seeds of a different sequence is also a potential problem, although most aggregation events tend to be sequence specific and mixed amyloids are relatively rare.[1]

We have been engaged in molecular dynamics (MD) simulations in an attempt to map the early steps of amyloidosis for nearly 15 years. Recently we identified a novel structure in simulations of the prion protein, lysozyme variants, transthyretin, and β_2-microglobulin under amyloidogenic conditions. Transthyretin deposits cause senile systemic amyloidosis and familial amyloid polyneuropathy,[10] dialysis and hereditary renal amyloidosis is associated with β_2-microglobulin,[11] lysozyme has been implicated in autosomal dominant hereditary amyloidosis,[12] and the prion protein is responsible for transmissible spongiform encephalopathies, including Creutzfeld–Jakob disease and bovine spongiform encephalopathy.[13]

All of these proteins have different native structures (Figure 1). Also, in all cases amyloidosis appears to proceed via partial unfolding, often through the low-pH endocytic pathway, with restructuring of the protein into an amyloidogenic intermediate, which then aggregates. In the course of studying the pH-induced partial unfolding of these proteins individually, we noticed that they all populated an unfolding intermediate with a novel secondary structure, α-sheet (Figure 1).[14–16] Since that time, we also observed this novel structure in polyglutamine,[17] which is implicated in Huntington's disease. The α-sheet structure is observed in all amyloidogenic proteins we have studied to date, while it is rare in other proteins and even in amyloidogenic proteins under normal conditions. Furthermore, the position of α-sheet within the sequence is correlated with the most amyloidogenic regions as determined experimentally.[14] The α-sheet is a possible backbone conformation that may explain the observations

Valerie Daggett received her B.A. in chemistry from Reed College in 1983. She attended the University of California, San Francisco, from 1985 to 1990, obtaining her Ph.D. under Peter Kollman and Tack Kuntz. Subsequently, she was a postdoctoral fellow at Stanford with Michael Levitt. She then joined the faculty of the University of Washington in 1993.
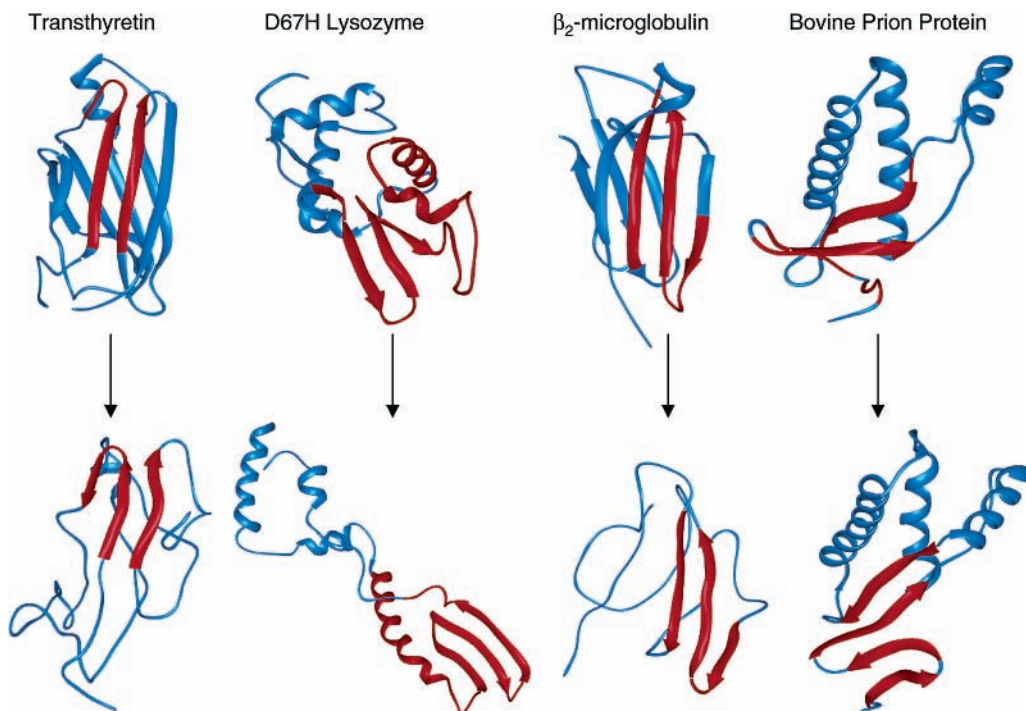
FIGURE 1. Native crystal structures for four amyloidogenic proteins (top) and their conversion to α-sheet (red strands, lower structures) during MD simulations at low pH with all native disulfide bonds intact.

discussed above regarding the toxic conformer detected with the conformation-specific antibody discussed above.

2. α-Sheet Structure

2.1. What Is α-Sheet? α-Sheet secondary structure is formed by regular hydrogen bonding between adjacent strands in the "α-extended chain" conformation. Rather than being formed by average repeating (ϕ,ψ) angles, as with the α-helix and β-strand, the α-extended chain conformation is defined by an alternation of residues in the right-handed (α_R) and the left-handed (α_L) helical conformations (Figure 2). While each residue is locally defined as helical, the alternation leads to formation of an extended sheet. This structure contains glide plane symmetry such that $\Phi_i = -\Phi_{i+1}$ and $\Psi_i = -\Psi_{i+1}$.

The average (ϕ,ψ) angles over the α-sheet structures obtained in multiple simulations of transthyretin, β_2-mircroglobulin, prion protein, and lysozyme were calculated: $\alpha_L = (45° \pm 8°, 92° \pm 28°)$ and $\alpha_R = (-87° \pm 7°, -49° \pm 4°)$. These angles do not correspond exactly to ideal values for the helical α_L or α_R conformations. According to the program PROCHECK,[18] our α_L-conformation is in an "additionally allowed" region and our α_R-conformation is in a "most favored" region. This is notable. So, while it may appear to be a strange structure, these angles are not in forbidden regions of the Ramachandran plot; in fact, short stretches of α-strands are populated in the Protein Data Bank (PDB)[19] of native structures.

2.2. α-Sheet Hydrogen Bonding. Figure 3 shows the native β-sheet hydrogen bond network from one face of the β-sandwich of the transthyretin crystal structure and the same sheet after conversion to α-sheet during the MD simulations.[15] Bifurcated hydrogen bonds can be important in the formation and stabilization of α-sheet structure. In Figure 3, the mode of bifurcation shown in light blue between the A- and G-strands was more prevalent. The hydrogen bonds in parallel and antiparallel β-sheets cannot participate in bifurcated hydrogen bonds, while an helix can be bifurcated between α-helical (i, $i + 4$), 3_{10}-helical (i, $i + 3$), and π-helical (i, $i + 5$) structure.[20]

2.3. Formation of α-Sheet Secondary Structure. The β-sheet → α-sheet transition illustrated in Figure 3 occurs sequentially through individual transitions of backbone (ϕ,ψ) angles in the various simulations, rather than all at once in a concerted manner. Such a crankshaft-like motion involves rotation of the peptide plane, changing the (ϕ,ψ) angle of residues i and $i + 1$, with only a minor change in the orientation of the side chains.[15,21]

In the transthyretin sheet shown in Figure 3, the β-sheet → α-sheet transition proceeded via sequential "peptide-plane flipping" starting on the AG-strands, moving on to the H-strand. This conversion occurs at both physiological and elevated temperature, the process is just much slower at lower temperature, requiring long simulation times to see the transition. The conversion process is akin to a domino-like effect that propagates across the sheet so that repulsive interactions are minimized. Alternatively, the residue flips back if the environment is not conducive to the transition. While there appears to be a preference for the direction of the flips in this sheet of the sandwich, the other sheet of TTR (not shown) flips in both directions, but many more simulations are necessary
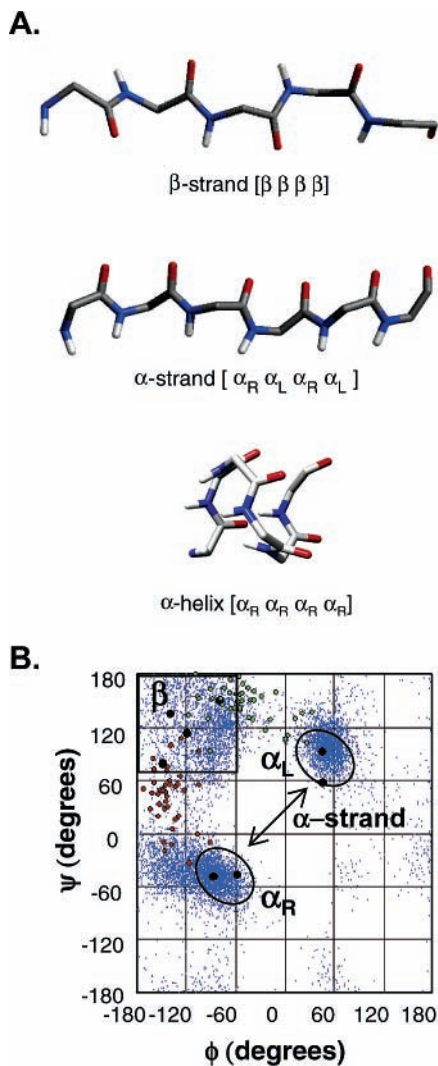
A.

β-strand [β β β β]

α-strand [α_R α_L α_R α_L]

α-helix [α_R α_R α_R α_R]

B.

FIGURE 2. α-Sheet structure: (A) main chain structures showing β-strands, α-strands, and α-helices; (B) positions of the underlying local conformations of these structures on a Ramachandran map. The red and green dots show the path of transitions from β-strand to α-strand occurring for two neighboring residues.

to determine whether such discrimination is statistically significant.

The conversion to α-sheet in monomeric TTR has also been observed by another group using a different force field and modeling program.[22] This same group reported earlier that they could not reproduce our results in their very short 1.8 ns simulations lacking explicit solvent.[23] However, when they used a more realistic representation of the system through inclusion of water and longer simulation times, they did indeed obtain results similar to ours.[15]

3. Historical Background of the α-Sheet

Unbeknownst to us when we first "discovered" α-sheet in our MD simulations, Pauling and Corey in fact predicted the structure in 1951.[24] They called it the "pleated sheet" and later the polar pleated sheet.[25] They proposed the α-sheet structure before outlining the details of parallel

and antiparallel β-pleated sheet structures, although the existence of β-sheets seems to have been accepted at the time based on Astbury's work.[26] Both the α- and β-sheets have the same meridonal repeat distance, 4.75 Å, and the same average hydrogen bond distance (2.3 Å). Pauling and Corey described three α-pleated sheets: one that was flat, one with a 7° rotation, and another with a 20° rotation.[24] Their flat α-sheet had $(\phi_1, \psi_1, \phi_2, \psi_2) = (-73°, -82°, 73°, 82°)$, the 7° rotation had $(\phi_1, \psi_1, \phi_2, \psi_2) = (-69°, -74°, 60°, 83°)$, the 20° rotation had $(\phi_1, \psi_1, \phi_2, \psi_2) = (-97°, -66°, 56°, 106°)$. For comparison, our average (ϕ, ψ) angles from MD are most similar to the Pauling and Corey model with 20° rotation, although we have observed all of these α-sheet conformations.

Pauling and Corey suggested that their pleated sheet was the primary extended structure in β-keratins because of the good agreement with fiber diffraction results.[27] After investigating the various predicted structures and comparing their energetic properties, they rightly came out in favor of β-sheets over α-sheets in "normal" proteins.[25] They reached this conclusion mainly because the polar pleated sheet was not a minimum in their dihedral potential function and the more stable α-sheet conformation in their force field led to a shorter residue chain distance, which did not agree with the fiber diffraction data as well as the β-sheet. They then evaluated both parallel and antiparallel β-sheets and concluded that they would be the dominant extended structure in proteins and that they would be less stable flat and more stable with a slight rotation between sheets. This was borne out, β-sheets usually exhibit a 15° rotation between strands, both in protein structures and in the cross β-structure of highly ordered amyloid fibrils,[2,28] but flat sheets (1.0−2.5°) have recently been observed in amyloid fibrils in 3D reconstructions from electron crystallography.[29,30]

Because α-sheet structure was dismissed by Pauling and Corey, it has not received much attention in the protein world since its original proposal; however, α-sheet has attracted attention in the "nonnatural" small peptide community. In particular there has been much interest in alternating D-,L-amino acids and "nonnatural" residues found in peptide antibiotics and ionophores. Given the relative preference for α_R configurations for L-amino acids and α_L for D-amino acids it was noted that in addition to helical structure sheet structures can form, particularly α-sheet.[31−33] Furthermore, it was concluded that for truly alternating D-/L-peptides the α-sheet was preferred. Heitz et al.[33] studied several such peptides and observed chain repeat distances by diffraction in good agreement with α-sheet. Interestingly, their IR spectra were very similar to those obtained for more conventional cross-β-structures for all L-polypeptides. This result is surprising and yet to be explained; we might expect a shift in the peaks for α-sheet due to the differences in hydrogen bonding.

More definitive demonstration of α-sheet came some time later when DiBlasio et al.[34] presented a crystal structure for a capped tripeptide (Boc-L-Ala-D-aIle-L-Ile-OMe) with $\Phi_1 = -75°$, $\Psi_1 = -26°$ and $\Phi_2 = 67°$, $\Psi_2 = 44°$. The third residue was shifted further from ideal values
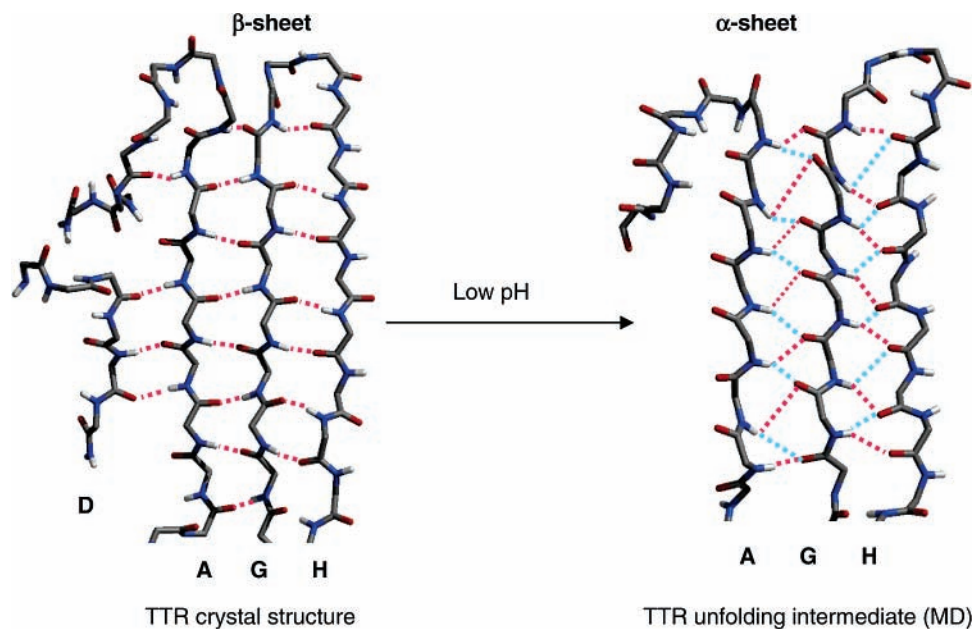
FIGURE 3. The DAGH β-sheet from the transthyretin crystal structure and after MD at low pH.

with $\Phi_1 = -105°$, $\Psi_1 = 16°$, but its NH and C=O groups remain aligned with its neighbors. The peptides form intermolecular antiparallel α-sheets in the crystal with some bifurcated hydrogen bonds. This was the first atomic-level proof for α-sheet. Later similar local α-strand conformations were detected in crystal structures of tripeptides with Cαα-diphenylglycine and α-aminoisobutyric acid,[35] as well as capped α−α-dicyclopropylglycine dipeptides.[36] These peptide studies demonstrate that α-strands and α-sheets do indeed exist and are not just theoretical or computational artifacts.

4. Evidence for α-Sheet Structure in Native Proteins

Since α-sheet structure appears to represent a novel form of secondary structure, it is important to see whether such structure is observed in experimentally determined protein structures. To this end, we searched the PDB[19] for examples of peptide segments (three residues or greater) that exhibit the characteristic alternation of residues in (+,+) and (−,−) conformational space (Schaeffer and Daggett, unpublished). There are 924 unique entries in this database that adopt such structure [924 of 29 936 total unique crystal and NMR structures, that is, each protein is only counted once when there are multiple NMR structures], and there are 1161 occurrences of α-strands in these 924 structures. Of these 1161 occurrences, 1093 are three-residue stretches, 67 contain four-residues, and one has five residues. There are not any occurrences of *bone fide* sheets. These numbers are different from what we published earlier (48 occurrences of four residues or more) for two main reasons: (1) our earlier calculation used the reduced nonredundant PDB, which only contained 5951 structures, and (2) we tightened our dihedral cutoffs to be considered α-sheet to within 35° (we used

45° previously) of the average values, which offsets the effect of the larger data set.

While NMR structures make up 15% of the structures evaluated, they represent 67% of the α-strands in the PDB. The α-strands in many of these NMR structures reside in poorly resolved N- or C-terminal regions of the protein, and they are therefore questionable. However, there are many NMR and crystal structures that contain well-defined α-strand conformations; we focus here on the crystal structures. In particular, lysozyme is an interesting case; consider two crystal structures of hen egg white lysozyme, 1HF4, 1.45 Å resolution,[37] and 1XEJ, 2.1 Å resolution.[38] Both of these structures contain a fairly long α-strand, comprising residues 72−75 in the first case and 71−75 in the second (Figure 4A). In fact, a neighboring proline also contributes its carbonyl group to the strand. What really makes this region interesting, though, is that mutation of Asp67 in the human protein to histidine (residue 66 in the hen numbering scheme) causes autosomal dominant hereditary amyloidosis. This residue is near the α-strand and, in fact, the region around residue 67 (residues 65−69) converts to α-strand in the MD simulations of the D67H human variant,[14] in addition to other residues C-terminal to the α-strand in the native state (residues 76−95). A short α-strand is also seen in this region in a human crystal structure, thereby leaving the protein poised to convert under amyloidogenic conditions. Residues 53−100 have been mapped to the core of protofibrils formed from conversion of hen egg white lysozyme.[39] These same residues form the core of an oligomeric model constructed using an MD-generated α-sheet intermediate of D67H lysozyme (Figure 4B). The core of this structure is very similar to the crystal structure of the fibrillar form of a seven-residue peptide from the yeast prion Sup35 by Eisenberg and co-workers.[40]
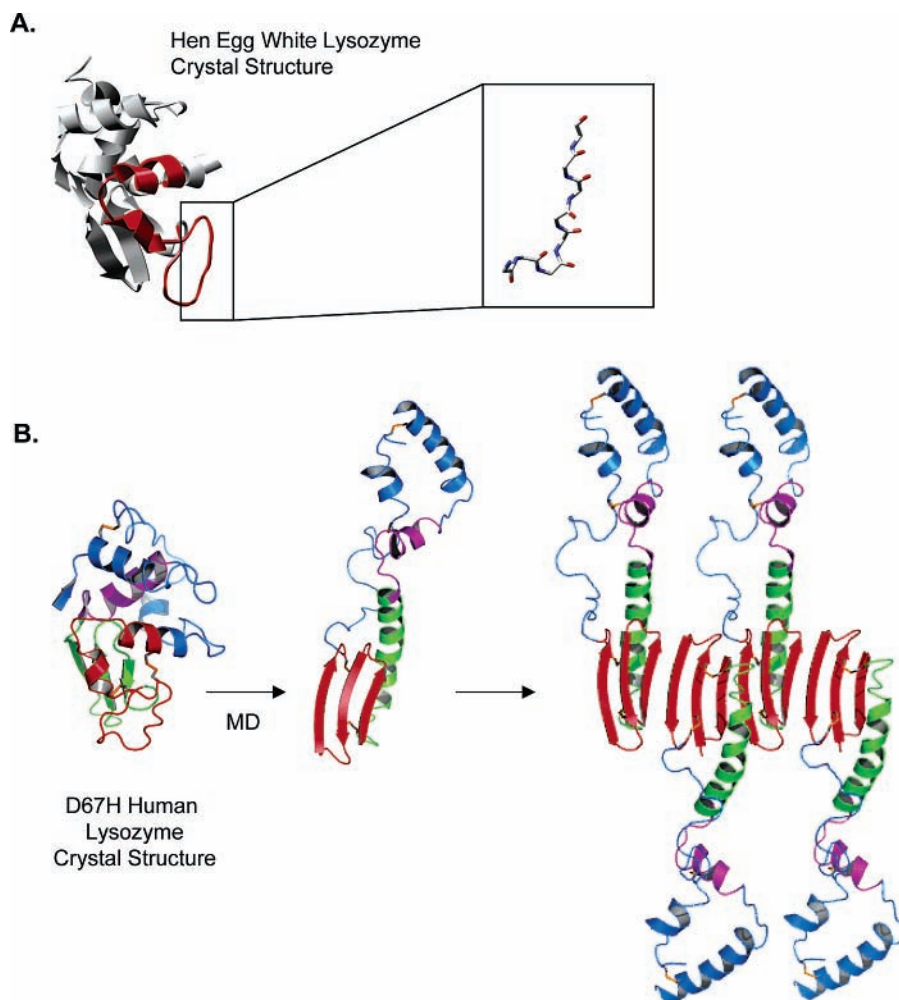
FIGURE 4. α-Strand and α-sheet structure in lysozyme: (A) α-strand structure in hen egg white lysozyme crystal structure; (B) conversion to α-sheet in MD simulation of human variant at low pH and a model of an α-sheet aggregate.

So, while rare in native structures, α-strands and sheets are observed. The bifurcated hydrogen bonding shown in Figure 3 is also observed in crystal structures, although it is much less extensive. The β-bulge of the C2 domain of synaptotagmin I (1rsy, 1.9 Å)[41] provides a nice example of this (Figure 5A). Thus, alternating α_L/α_R conformations are not only in allowed regions of conformational space, they are populated in native states. The importance of α-strands to function is also evident by their role in binding K^+ in the potassium channel (1bl8, 3.2 Å, Figure 5B).[42] Furthermore, a recent study of protein structures in the PDB has shown that a short alternation of the α_R and the α_L can create anion and cation binding site "nests".[43,44]

6. Potential α-Sheet Structure in Fibrils

It is our hypothesis that α-sheet forms in amyloidogenic intermediates and the resulting soluble oligomers. If so, then the question is whether α-sheet is carried through to the mature fibrils or conversions to β-sheet occur. It is possible that α-sheet secondary structure is only formed in the prefibrillar amyloidogenic intermediate, because several recent experiments suggest that highly ordered amyloid fibrils of peptides are composed of both parallel

and antiparallel β-structure.[45,46] However, the β-structure per se is typically assumed, not determined directly. The structure is estimated by comparing the observed chemical shifts with the chemical shifts of model compounds/ proteins.[47] We have shown that the chemical shifts calculated for an α-sheet of transthyretin are very similar to those of the same residues in a β-sheet,[15,48] and both sets of calculated values are in agreement with solid-state NMR data.[49] In addition, the C−C and C−N distances determined by solid-state NMR can be satisfied by both α- and β-sheets. So, it may be premature to rule out α-sheet in the fibrillar form.

Amyloid fibrils, and all the species leading up to fibrils, are structurally very heterogeneous even under controlled in vitro conditions,[29] and the situation becomes even more complicated in vivo. Such heterogeneity (i.e., multiple conformations) has been linked to strain differences and species barriers in prion diseases. For example different variants can give rise to different amyloid conformations.[50] In the first such example of this, Caughey and co-workers[51] provided direct evidence for strain-dependent differences in the β-sheet conformations of the scrapie form of the prion protein by FTIR for material derived from mice with different phenotypes: hyper and drowsy. Interestingly, the
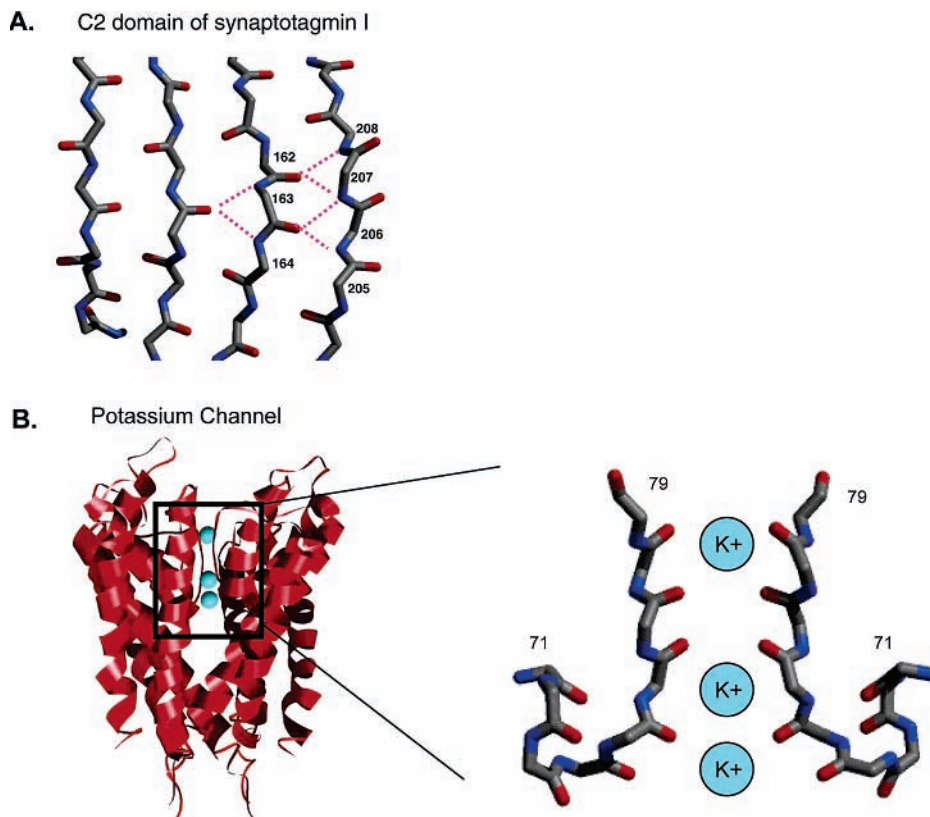
FIGURE 5. α-Strand and α-sheet structure in native crystal structures: (A) α-sheet along the edge of a β-sheet in the C2 domain of synaptotagmin I; (B) the potassium channel makes use of α-strands to bind K$^+$.

differences were in the type of sheet structure as opposed to the overall amount of structure. This provides an explanation for the contention that PrP^{Sc} serves as a template for conversion such that conformational diversity leads to different forms of endogenous, newly converted PrP^{Sc}.[52] Metal ions can also modulate the different PrP^{Sc} forms,[53] and metal binding by α-strands has been observed.

More recently the first direct biophysical evidence that protein conformations are transmitted in prion strains was reported by Jones and Surewicz.[54] They found that amyloids from different species adopt distinct secondary structures and morphologies and that cross-seeding with preformed fibrils of one species to another lead to a new strain that inherits the structure of the template seed. In this way, strain and species barriers are inextricably linked via conformation. Such results are typically interpreted in terms of alterations in β-structure (and ultimately how the sheets pack determine the morphology). We suggest that α-sheet may also help account for this heterogeneity and mixed α- and β-sheet structures should also be considered.

In addition to observations of different β-sheet structures by FTIR, some unusual amide I bands have been observed that deviate from bands known to reflect β-structure. For example, Lopez de la Paz et al.[55] observed a prominent peak at 1595 cm^{-1}. They were unable to explain the physical basis of this peak except to speculate that it might arise from protofilament packing. Zurdo et al.[56] observed a similar peak in soluble oligomers with band

shifts to the more characteristic 1620 cm^{-1} wavelength for the mature, purified fibrils. Zandomeneghi et al.[57] also recently described the distinction in the FTIR spectra for native β-sheet proteins and amyloid fibrils. It may be that the more amorphous oligomers with the anomalous FTIR peak reflect α-sheet structure, as we might expect a shift to lower wavenumbers for this structure given the differences in hydrogen bonding and molecular dipole.

7. α-Sheet Intermediates in Amyloid Disease

The most striking characteristic of α-sheet structure is the alignment of the carbonyl and amide groups participating in hydrogen bonds between the strands forming a "polar pleated sheet". This particular alignment of peptide groups also explains the hydrogen exchange protection patterns observed for the amyloidogenic forms of transthyretin and β$_2$-microglobulin, as well as the lack of protection observed for many amides that should be protected in a β-sheet.[15,16]

Figure 6 shows how the partial charges from the peptide backbone conformation create two complementary charged interfaces. Arnsdorf and co-workers have suggested that amyloidogenic proteins build up a molecular dipole at low pH and that attractive forces between dipoles account for their linear self-assembly.[58] Their model focuses on interactions between charged side chains, but we propose that the main chain is critical. In any case, the α-sheet scaffold may also catalyze the conversion of individual peptide groups to undergo pep-
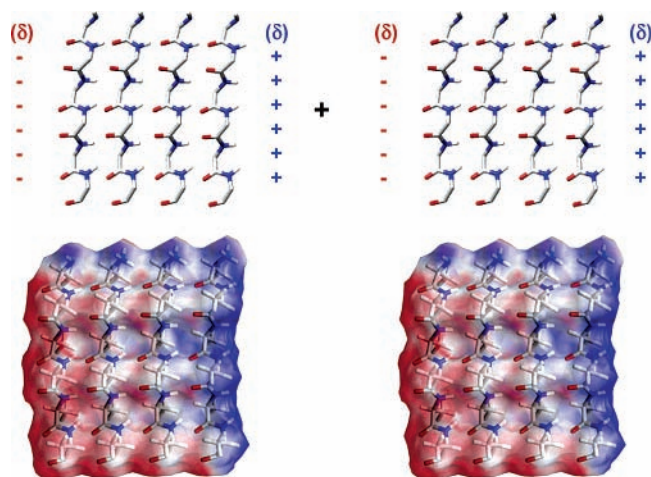
FIGURE 6. Schematic representation of how electrostatic complementarity between two (in this case identical) α-sheets may facilitate oligomerization.

tide plane flips and align with the overall molecular dipole to form α-sheet if they approach in an alternative conformation. In contrast to β-structure, the peptide groups in α-sheet share a similar orientation, as with the α-helix. The arrangement of the planar peptide groups in an α-helix contributes to a greater total magnetic anisotropy for α-helices compared with β-sheets.[59,60] A similar phenomenon in the α-sheet may explain why amyloid fibrils grow more efficiently and in an ordered orientation in the presence of a magnetic field,[61,62] as well as aligning parallel to the magnetic field like α-helices.[59]

We propose that as an amyloidogenic protein unfolds, α-sheet structure facilitates self-association into soluble oligomeric amyloid protofibrils. An intriguing observation that supports the idea of non-β-sheet structure in the oligomers is that there is no evidence of β-structure in the lag phase of aggregation of polyQ and Aβ although soluble oligomers are detected.[63–66] If the soluble protofibrils are formed via an α-sheet intermediate, the transition from α- to β-sheet may become increasingly more favorable as the protofibrils undergo a transition from the toxic soluble polar phase to the insoluble more highly ordered amyloid fibrils. Alternatively, α-sheet may remain in the mature fibrils. Given the antibody that preferentially binds protofibrils and amyloidogenic intermediates but not mature fibrils, the scenario in which α-sheet converts to β-sheet as the fibril matures seems most likely for most proteins. However, α-sheet is compatible with solid state NMR observables for amyloid fibrils,[15] suggesting that it is possible that it is present in mature fibrils. Hopefully both experimental and theoretical studies in the future will be able to distinguish between these possibilities. Another consideration is that amyloid fibrils can be very heterogeneous with respect to structure, as discussed above; it's possible that both α- and β-sheet are present depending on the sequence and conditions.

Experiments also provide insight into how subunits are arranged in fibrils.[67,68] Fiber diffraction[67–69] and X-ray crystallographic experiments[40,46] indicate that the amyloid fibril structure is not β-helix and instead is made up of

conventional packed sheets.[28] Our models involving conversion to sheetlike structure and subsequent oligomerization, with often relatively minor alterations of the native topology, are consistent with what one would expect en route to stacked-sheet fibrils.[70]

That some peptide fragments are more amyloidogenic than others suggests that there is a sequence propensity for amyloid formation. While the main chain configuration presented by α-sheet structure is the same for different sequences, individual amino acids have different propensities for α-sheet. The sequence rules governing amyloid formation are being systematically mapped,[71,72] and consideration of α-sheet structure may provide an improved understanding of this process and avenues for intervention.

Conclusions

We propose that a relatively obscure structure, the α-sheet, may represent the toxic conformer in amyloid diseases. This structure nicely explains a number of experimental observations, but at this point, it is a hypothesis. Further work is necessary, and ongoing, to develop stable α-sheet peptides to determine the biophysical signatures of the structure. With such information in hand, one can begin to more directly test for the existence and role of α-sheet in amyloidosis.

References

(1) Westermark, P. Aspects on human amyloid forms and their fibril polypeptides. *FEBS J.* **2005**, *272*, 5942–5949.
(2) Blake, C.; Serpell, L. Synchrotron X-ray studies suggest that the core of the transthyretin amyloid fibril is a continuous beta-sheet helix. *Structure* **1996**, *4*, 989–998.
(3) Hardy, J.; Selkoe, D. J. The amyloid hypothesis of Alzheimer's disease: Progress and problems on the road to therapeutics. *Science* **2002**, *297*, 353–356.
(4) Bucciantini, M.; Giannoni, E.; Chiti, F.; Baroni, F.; Formigli, L.; Zurdo, J. S.; Taddei, N.; Ramponi, G.; Dobson, C. M.; Stefani, M. *Nature* **2002**, *416*, 507–511.
(5) Silveira, J.; Raymond, G. J.; Hughson, A. G.; Race, R. E.; Sim, V. L.; Hayes, S. F.; Caughey, B. The most infectious prion protein particles. *Nature* **2005**, *437*, 257–261.
(6) Bodner, R. A.; Outeiro, T. F.; Altmann, S.; Maxwell, M. M.; Cho, S. H.; Hyman, B. T.; McLean, P. J.; Young, A. B.; Housman, D. E.; Kazantsev, A. G. Pharmacological promotion of inclusion formation: A therapeutic approach for Huntington's and Parkinson's diseases. *Proc. Natl. Acad. Sci. U.S.A.* **2006**, *103*, 4246–4251.
(7) Kayed, R.; Head, E.; Thompson J. L.; McIntire, T. M.; Milton, S. C.; Cotman, C. W.; Glabe, C. G. Common structure of soluble amyloid oligomers implies common mechanism of pathogenesis. *Science* **2003**, *300*, 486-489.
(8) Glabe, C. G.; Kayed, R. Common structure and toxic function of amyloid oligomers implies a common mechanism of pathogenesis. *Neurology* **2006**, *66*, S74–S78.
(9) Lundmark, K.; Westermark, G. T.; Nystrom, S.; Murphy, C. L.; Solomon, A.; Westermark, P. Transmissibility of systemic amyloidosis by a prion-like mechanism. *Proc. Natl. Acad. Sci. U.S.A.* **2002**, *99*, 6979–6984.
(10) Saraiva, M. J. M. Transthyretin mutations in hyperthyroxinemia and amyloid diseases. *Hum. Mutat.* **2001**, *17*, 493–503.
(11) Inoue, S.; Kuroiwa, M.; Ohashi, K.; Hara, M.; Kisilevsky, R. Ultrastructural organization of hemodialysis-associated beta 2-microglobulin amyloid fibrils. *Kidney Int.* **1997**, *52*, 1543–1549.

(12) Pepys, M. B.; Hawkins, P. N.; Booth, D. R.; Vigushin, D. M.; Tennent, G. A.; Soutar, A. K.; Totty, N.; Nguyen, O.; Blake, C. C. F.; Terry, C. J.; Feest, T. G.; Zalin, A. M.; Hsuan, J. J. *Nature* **1993**, *362*, 553−557.

(13) Prusiner, S. B. Prions *Proc. Natl. Acad. Sci. U.S.A.* **1998**, *95*, 13363−13383.

(14) Armen, R. S.; DeMarco, M. L.; Alonso, D. O. V.; Daggett, V. Pauling and Corey's α-pleated sheet structure may define the prefibrillar amyloidogenic intermediate in amyloid disease *Proc. Natl. Acad. Sci. U.S.A.* **2004**, *101*, 11622−11627.

(15) Armen, R. S.; Alonso, D. O. V.; Daggett, V. Anatomy of an amyloidogenic intermediate: Conversion of β-sheet to α-pleated sheet structure in transthyretin at acidic pH. *Structure* **2004**, *12*, 1847−1863.

(16) Armen, R. S.; Daggett, V. Characterization of two distinct β2-microglobulin unfolding intermediates that may lead to amyloid fibrils of different morphology. *Biochemistry* **2005**, *44*, 16098−16107.

(17) Armen, R. S.; Bernard, B. M.; Day, R.; Alonso, D. O. V.; Daggett, V. Characterization of a possible amyloidogenic precursor in glutamine repeat neurodegenerative diseases. *Proc. Natl. Acad. Sci. U.S.A.* **2005**, *102*, 13433−13438.

(18) Laskowski, R. A.; Macarthur, M. W.; Moss, D. S.; Thornton, J. M. Procheck − a program to check the stereochemical quality of protein structures. *J. Appl. Crystallogr.* **1993**, *26*, 283−291.

(19) Berman, H. M.; Westbrook, J.; Feng, Z.; Gilliland, G.; Bhat, T. N.; Weissig, H.; Shindyalov, I. H.; Bourne, P. E. The Protein Data Bank. *Nucleic Acids Res.* **2000**, *28*, 235−242.

(20) Armen, R.; Alonso, D. O. V.; Daggett, V. The Role of α, 3_{10}, and π-helix in Helix → Coil Transitions. *Protein Sci.* **2003**, *12*, 1145−1157.

(21) Daggett, V.; Kollman, P. A.; Kuntz, I. D. Molecular Dynamics Simulations of Small Peptides: Dependence on Dielectric Model and pH. *Biopolymers* **1991**, *31*, 285−304.

(22) Yang, M.; Lei, M.; Yordanov, B.; Huo, S. Peptide plane can flip in two opposite directions: Implication in amyloid formation of transthyretin, *J. Phys. Chem. B* **2006**, *110*, 5829−5833.

(23) Yang, M.; Lei, M.; Bruschweiler, R.; Huo, S. Initial conformational changes of human transthyretin under partially denaturing conditions. *Biophys. J.* **2005**, *89*, 433−443.

(24) Pauling, L.; Corey, R. B. The pleated sheet, a new layer configuration of polypeptide chains. *Proc. Natl. Acad. Sci. U.S.A.* **1951**, *37*, 251−256.

(25) Pauling, L.; Corey, R. B. Configurations of polypeptide chains with favored orientations around single bonds: Two new pleated sheets. *Proc. Nat. Acad. Sci. U.S.A.* **1951**, *37*, 729−740.

(26) Astbury, W. T. Some problems in the X-ray analysis of the structure of animal hairs and other protein fibres. *Trans. Faraday Soc.* **1933**, *29*, 193−205.

(27) Pauling, L.; Corey, R. B. The structure of feather rachis keratin. *Proc. Natl. Acad. Sci. U.S.A.* **1951**, *37*, 256−261.

(28) Makin, O. S.; Serpell, L. C. Structures for amyloid fibrils. *FEBS J.* **2005**, *272*, 5950−5961.

(29) Jimenez, J. L.; Guijarro, J. L.; Orlova, E.; Zurdo, J.; Dobson, C. M.; Sunde, M.; Saibil, H. R. Cryo-electron microscopy structure of an SH3 amyloid fibril and model of the molecular packing. *EMBO J.* **1999**, *18*, 815−821.

(30) Jimenez, J. L.; Nettleton, E. J.; Bouchard, M.; Robinson, C. V.; Dobson, C. M.; Saibil, H. R. The protofilament structure of insulin amyloid fibrils. *Proc. Natl. Acad. Sci. U.S.A.* **2002**, *99*, 9196−9201.

(31) Hesselink, F. T.; Scheraga, H. A. Laser raman spectroscopy of polypeptides. II. Spectra of random poly(hydroxybutylglutamine-*co*-glycine) in the solid state. *Macromolecules* **1972**, *5*, 455.

(32) DeSantis, P.; Morosetti, S.; Rizzo, R. Conformational analysis of regular enantiomeric sequences. *Macromolecules* **1974**, *7*, 52−58.

(33) Heitz, F.; Detriche, G.; Vovelle, F.; Spach, G. Sheet structures in alternating poly(D,L-peptides). *Macromolecules* **1981**, *14*, 47−50.

(34) Di Blasio, B.; Saviano, M.; Fattorusso, R.; Lombardi, A.; Pedone, C.; Valle, V.; Lorenzi, G. P. A crystal structure with features of an antiparallel α-pleated sheet. *Biopolymers* **1994**, *34*, 1463−1468.

(35) Pavone, V.; Lombardi, A.; Saviano, M.; Nastri, F.; Zaccaro, L.; Maglio, O.; Pedone, C.; Omote, Y.; Yamanaka, Y.; Yamada, T. Conformational behaviour of C^{αα}-diphenylglycine: Folded vs extended structures in DΦG-containing tripeptides. *J. Pept. Sci.* **1998**, *4*, 21−32.

(36) De Simone, G.; Lombari, A.; Galdiero, S.; Nastri, F.; Di Costanzo, L.; Gohda, S.; Yamada, T.; Pavone, V. The crystal structure of a Dcp-containing peptide. *Biopolymers* **2000**, *53*, 182−188.

(37) Vaney, M. C.; Broutin, I.; Retailleau, P.; Douangamath, A.; Lafont, S.; Hamiaux, C.; Prange, T.; Ducruix, A.; Ries-Kautt, M. Structural effects of monovalent anions on polymorphic lysozyme crystals. *Acta Crystallogr., Sect. D* **2001**, *57*, 929−940.

(38) Nagendra, H. G.; Sukumar, N.; Vijayan, M. Role of water in plasticity, stability, and action of proteins: the crystal structures of lysozyme at very low levels of hydration. *Proteins* **1998**, *32*, 229−240.

(39) Frare, D.; Polverino de Laureto, P.; Zurdo, J.; Dobson, C. M.; Fontana, A. A highly amyloidogenic region of hen lysozyme. *J. Mol. Biol.* **2004**, *340*, 1153−1165.

(40) Nelson, R.; Sawaya, M. R.; Balbirnie, M.; Madsen, A. O.; Riekel, C.; Grothe, R.; Eisenberg, D. Structure of the cross-β spine of amyloid-like fibrils. *Nature* **2005**, *435*, 773−778.

(41) Sutton, R. B.; Davletov, B. A.; Berghuis, A. M.; Sudhof, T. C.; Sprang, S. R. Structure of the first C2 domain of synaptotagmin I: a novel Ca2+/phospholipid-binding fold. *Cell* **1995**, *80*, 929−938.

(42) Doyle, D. A.; Morais Cabral, J.; Pfuetzner, R. A.; Kuo, A.; Gulbis, J. M.; Cohen, S. L.; Chait, B. T.; MacKinnon, R. The structure of the potassium channel: molecular basis of K+ conduction and selectivity. *Science* **1998**, *280*, 69−77.

(43) Watson, J. D.; Milner-White E. J. A novel main-chain anion-binding site in proteins: The nest. A particular combination of phi,psi values in successive residues gives rise to anion-binding sites that occur commonly and are found often at functionally important regions. *J. Mol. Biol.* **2002**, *315*, 171−182.

(44) Watson, J. D.; Milner-White E. J. The conformations of polypeptide chains where the main-chain parts of successive residues are enantiomeric. Their occurrence in cation and anion-binding regions of proteins. *J. Mol. Biol.* **2002**, *315*, 183−191.

(45) Tycko, R. Solid-state NMR as a probe of amyloid fibril structure. *Curr. Opin. Chem. Biol.* **2000**, *4*, 500−506.

(46) Nelson, R.; Eisenberg, D. Recent atomic models of amyloid fibril structure. *Curr. Opin. Struct. Biol.* **2006**, *16*, 1−6.

(47) Cornilescu, G.; Delaglio, F.; Bax, A. Protein backbone angle restraints from searching a database for chemical shift and sequence homology. *J. Biomol. NMR* **1999**, *13*, 289−302.

(48) Xu, X. P.; Case, D. A. Automatic prediction of ^{15}N, ^{13}Cα, ^{13}Cβ, and ^{13}C′ chemical shifts in proteins using a density functional database. *J. Biomol. NMR* **2001**, *21*, 321−333.

(49) Jaroniec, C. P.; MacPhee, C. E.; Astrof, N. S.; Dobson, C. M.; Griffin, R. G. Molecular conformation of a peptide fragment of transthyretin in an amyloid fibril. *Proc. Natl. Acad. Sci. U.S.A.* **2002**, *99*, 16748−16753.

(50) Ross, E. D.; Edskes, H. K.; Terry, M. J.; Wickner, R. B. Primary sequence independence for prion formation. *Proc. Natl. Acad. Sci. U.S.A.* **2005**, *102*, 12825−12830.

(51) Caughey, B.; Raymond, G. J.; Bessen, R. A. Strain-dependent differences in beta-sheet conformations of abnormal prion protein. *J. Biol. Chem.* **1998**, *273*, 32230−32235.

(52) Telling, G. C.; Parchi, P.; DeArmond, S. J.; Cortelli, P.; Montagna, P.; Gabizon, R.; Mastrianni, J.; Lugaresi, E.; Gambetti, P.; Prusiner, S. B. *Science* **1996**, *274*, 2079−2082.

(53) Wadsworth, J. D.; Hill, A. F.; Joiner, S.; Jackson, G. S.; Clarke, A. R.; Collinge, J. Strain-specific prion-protein conformation determined by metal ions. *Nat. Cell. Biol.* **1999**, *1*, 55−59.

(54) Jones, E. M.; Surewicz, W. K. Fibril conformation as the basis of species- and strain-dependent seeding specificity of mammalian prion amyloids. *Cell* **2005**, *121*, 63−72.

(55) Lopez de la Paz, M.; Goldie, K.; Zurdo, J.; Lacroix, E.; Dobson, C. M.; Hoenger, A.; Serrano, L. *De novo* designed peptide-based amyloid fibrils. *Proc. Natl. Acad. Sci. U.S.A.* **2002**, *99*, 16052−16057.

(56) Zurdo, J.; Guijarro, J. I.; Dobson, C. M. Preparation and characterization of purified amyloid fibrils. *J. Am. Chem. Soc.* **2001**, *123*, 8141−8142.

(57) Zandomeneghi, G.; Krebs, M. R. H.; McCammon, M. G.; Fandrich, M. FTIR reveals structural differences between native β-sheet proteins and amyloid fibrils. *Protein Sci.* **2004**, *13*, 3314−3321.

(58) Xu, S. H.; Bevis, B.; Arnsdorf, M. F. The assembly of amyloidogenic yeast Sup35 as assessed by scanning (atomic) force microscopy: An analogy to linear colloidal aggregation? *Biophys. J.* **2001**, *81*, 446−456.

(59) Worchester, D. L. Structural origins of diamagnetic anisotropy in proteins. *Proc. Natl. Acad. Sci. U.S.A.* **1978**, *75*, 5475−5477.

(60) Pauling, L. Diamagnetic anisotropy of the peptide group. *Proc. Natl. Acad. Sci. U.S.A.* **1979**, *76*, 2293−2294.

(61) Fraser, P. E.; Duffy, L. K.; O'Mally, M. B.; Nguyen, J.; Inouye, H.; Kirschner, D. A. Morphology and antibody recognition of synthetic beta-amyloid peptides. *J. Neurosci. Res.* **1991**, *28*, 474−485.

(62) Malinchik, S. B.; Inouye, H.; Szumowski, K. E.; Kirschner, D. A. Structural analysis of Alzheimer's beta (1−40) amyloid: Protofilament assembly of tubular fibrils. *Biophys. J.* **1998**, *74*, 537−545.

(63) Huang T. H. J.; Yang D. S.; Fraser P. E.; Chakrabartty, A. Alternate aggregation pathways of the Alzheimer beta-amyloid peptide − An in vitro model of preamyloid. *J. Biol. Chem.* **2000**, *275*, 36436−36440.

(64) Chen, S.; Ferrone, F. A.; Wetzel, R. Huntington's disease age-of-onset linked to polyglutamine aggregation nucleation. *Proc. Natl. Acad. Sci. U.S.A.* **2002**, *99*, 11884−11889.

(65) Gorman, P. M.; Yip, C. M.; Fraser, P. E.; Chakrabartty, A. Alternate aggregation pathways of the Alzheimer beta-amyloid peptide: A beta association kinetics at endosomal pH. *J. Mol. Biol.* **2003**, *325*, 743−757.

(66) Kim, J. R.; Muresan, A.; Lee, K. Y. C.; Murphy, R. M. Urea modulation of beta-amyloid fibril growth: Experimental studies and kinetic models. *Protein Sci.* **2004**, *13*, 2888−2898.

(67) Sunde, M.; Serpell, L. C.; Bartlam, M.; Fraser, P. E.; Pepys, M. B.; Blake, C. C. F. Common core structure of amyloid fibrils by synchrotron X-ray diffraction. *J. Mol. Biol.* **1997**, *273*, 729−739.

(68) Nguyen, J. T.; Inouye, H.; Baldwin, M. A.; Fletterick, R. J.; Dohen, F. E.; Prusiner, S. B.; Kirschner, D. A. X-ray diffraction of scrapie prion rods and PrP peptides. *J. Mol. Biol.* **1995**, *252*, 412−422.

(69) Wang, J.; Gülich, S.; Bradford, C.; Ramirez-Alvarado, M.; Regan, L. A Twisted four-sheeted model for an amyloid fibril. *Structure* **2005**, *13*, 1279−1288.

(70) DeMarco, M. L.; Daggett, V. From conversion to aggregation: Protofibril formation of the prion protein. *Proc. Natl. Acad. Sci. U.S.A.* **2004**, *101*, 2293−2298.

(71) Lopez de la Paz, M.; Serrano, L. Sequence determinants of amyloid fibril formation. *Proc. Natl. Acad. Sci. U.S.A.* **2004**, *101*, 87−92.

(72) Thompson, M. J.; Sievers, S. A.; Karanicolas, J.; Ivanova, M. I.; Baker, D.; Eisenberg, D. The 3D profile method for identifying fibril-forming segments of proteins. *Proc. Natl. Acad. Sci. U.S.A.* **2006**, *103*, 4074−4078.

AR0500719